

A NEW METHOD TO DETERMINE RIB GEOMETRY FOR A PERSONALISED FEM OF THE THORAX

O. Mayeur^{a,b,c}, F. Chaari^{a,b,c}, R. Delille^{a,b,c}, H. Guillemot^{a,b,c}, P. Drazetic^{a,b,c}

^aUniv Lille Nord de France, F-59000 Lille, France

^bUVHC, LAMIH, F-59313 Valenciennes, France

^cCNRS, FRE 3304, F-59313 Valenciennes, France

ABSTRACT

The thorax is one of the segments frequently involved in road accidents. Various models of the human chest have been published to evaluate injury risks or to access innovative safety systems. The purpose of this study is to determine relevant parameters of the human ribcage (cortical thicknesses, cross section inertia...) to enrich FE models. This original method has been developed by combining CT-scan, 3D laser scan and µCT-scan to determine precisely the internal rib architecture. The main advantage of this approach is to provide a FE model which is personalised, biofidelic and taking into account both geometry and bone distribution.

Keywords: Thorax, Computer Aided Design, Crashworthiness, Models.

I- INTRODUCTION

Despite of a broad decrease in road accident occurrence in developed countries during the past years, this health issue remains a concern in developing countries and even at a worldwide scale. A recent study issued by the World Health Organization (WHO, 2004; WHO, 2009a) reported that road accidents will be the third cause of premature deaths in 2020. Moreover, at the end of 2009, WHO declared the decade 2011-2020 as the “Decade of Action for Road Safety” (WHO, 2009b). Besides these general considerations, research aiming at improving road safety is still needed to provide advanced numerical tools for future evaluations of new cars – particularly for self certification, to develop innovative safety designs, and to harmonise consumerism assessments. This approach globally known as Virtual Testing (VT) is sustained internationally by recently constituted workgroups like WG22 of the European Enhanced Vehicle-safety Committee (EEVC), SC10-SC12/WG4 of the International Standard Organization (ISO), international initiatives like the Global Human Body Modelling Consortium (GHBMC), and research projects supported by the European Commission like THOMO or THORAX. One of the common tasks of all these projects is to describe as accurately as possible the geometry of the human body, not only at a global level, but also at a microscopic scale to define parameters as inputs for new generation finite element models. Indeed, due to computer progress, new generation models move towards a more and more refined definition of the constitutive body parts, which would enable providing highly detailed geometry of the human body.

Numerous models of the human body have already been populated. Labman (Lizee, 1998), Thums (Iwamoto, 2002), Humos 1 (Robin, 2001) and 2 (Behr, 2003), were published as incomes of European consortiums or as car manufacturer initiatives. Although the geometry of all these projects came from CT images, they suffered from a lack of precision regarding the microscopic description of the constitutive parts, and were constrained by simplification needed for global testing, element number limitations, or computer capabilities. Consequently, these models were limited in their biofidelity and needed parameter identification to fit the available experimental datasets.

The thorax is one of the segments frequently involved in road accidents (Foret-Bruno, 1998; Foret-Bruno, 2001). Among the numerous models of the human body evoked above, including the chest, most have been published over the past decade to study injury mechanisms, to evaluate injury risks in

car collisions and to access innovative safety systems. More recently, experimental investigations have been conducted to access detailed characteristics of the human ribcage. The main motivation was to overpass the limits described above and therefore to provide models an accurate description of the cortical bone thickness of the ribs, which is a major factor influencing the thorax response submitted to an impact (Kemper, 2007; Sandoz, 2007; Trosseille, 2008). Previous studies investigated this parameter by using physical measurements (Roberts, 1972), photographs (Yoganandan, 1998; Kallieris, 2000), medical CT-scans (Kent, 2005) or vet CT-scans (Charpail, 2005). An original work, conducted thanks to a micro CT, has also been proposed by Li (Li, 2009). Particularly, it has been demonstrated that CT images issued from clinical acquisitions are not sufficient to measure precisely the cortical bone thickness; indeed, the lowest resolution available is usually 0.6 to 0.8 mm, whilst the thickness of the cortical bone is frequently thinner than 1 mm. Thus, the characterisation of the thorax geometry at a multilevel scale requires multiple acquisition devices to be secondarily merged to build a complete model.

The purpose of this study is to propose a new method to determine relevant parameters of the human ribcage to be incorporated in a refine FE model. This original method has been developed by combining medical CT images, 3D laser scan acquisitions, and micro-CT techniques to determine precisely the internal rib architecture within the entire ribcage geometry. All these data were merged to define a geometrical thorax model at a multilevel scale (thorax, rib, bone structure). At the end, a finite element model was built from this complete geometrical acquisition as a feasibility step to access the quality of the meshing obtained.

II- METHOD

II.1- DATA ACQUISITION

The geometry of the whole thorax was obtained precisely at 3 different scales, by using successively 3 acquisition systems: first, the whole geometry of the thorax was acquired with a medical CT scanner; at a lower level, the external geometry of all ribs was recorded with a contactless 3D laser scanner; finally, the structural geometry of ribs (i.e. spongy and cortical bone) was defined on 35 mm in length samples digitized in a micro CT scanner (μ CT).

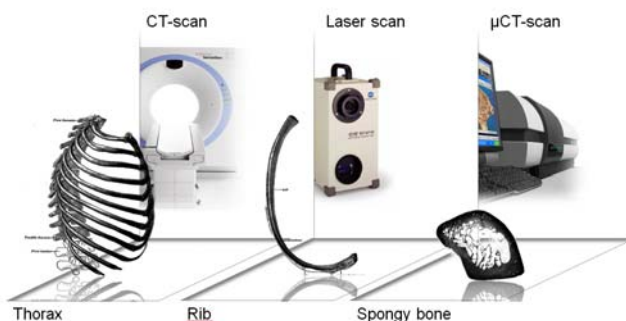


Fig. 1 - Acquisition Devices and Corresponding Imaging Scales.

The present study was performed - as a feasibility step within the framework of the project THOMO - on the 7th right rib of a PMHS submitted to a left side impact at CEEsar. The subject, a 92 year old male, was supplied to the project by the Body Donation program of the University of Paris with respect to ethical rules and a scientific committee approval. The body was frozen in an upright position to fix the ribs, the spine, and the internal organs in an anatomical position close to live beings. The work presented in this paper describes the protocol applied on one rib as a feasibility step to be later applied on a whole thorax.

The first step consists of obtaining, prior to testing, at macroscopic level, the global geometry of the thorax using a medical CT scan, thanks to collaboration between CEEsar, Hôpital Cochin

Radiologie B, ENSAM and LAB. DICOM slices were acquired on a CT-Scan Siemens Sensation 16 (120 kV, 155 mA) with a 512 x 512 matrix of 0.934 mm pixels. The interval between slices was defined as 0.8 mm without overlap, and the field of view was limited to 47.80 cm. The image reconstruction was done with a B70f algorithm (Convolution Kernel) corresponding to bone tissues.

After the lateral impact delivered on the left side of the thorax, right ribs were harvested from the thorax for the second step. Each rib was then positioned in front of a Konica Minolta (VIVID 910) laser scanner. A detailed description of this technique with its principle and the resolution (about $\pm 0.1\text{mm}$) used can be found in a previous publication (Delille, 2007). Solid lines were drawn with a surgical marker every 35 mm along the rib to define section cuts to be done for step 3. These marks were visible on the 3D laser acquisition and thus allowed repositioning afterward the 3D models from the μCT scanner (step 3) on our model medical imaging (step 1). The samples were defined as 35 mm long as the μCT scanner allows scanning samples with a maximal size of 40 mm height. For this particular study, the 7th rib was divided in 8 sections.

The third step, at a microscopic level, regards the scanning of samples in the μCT scanner to obtain the structural geometry: this step allows differentiating the cortical bone from the spongy bone. μCT scanning was performed thanks to a 1172 SKYSCAN system, with 80 kV and 100 μA settings. The voxel size for all μCT data was adjusted to 20.8 μm . This choice was conditioned by the complexity of the whole 3D model and the acquiring time: under these conditions, the duration of acquisition is about 2 hours for a sample of 35mm height.

Once these three acquisition steps achieved, a set of different data of the same geometry at different scales and coordinate systems have to be merged in order to build the whole geometrical model of human thorax.

II.2- GEOMETRICAL MODEL RECONSTRUCTION

The positioning of all scan data is made in 2 steps, in a bottom-up scheme: from μCT to 3D laser reconstruction and then to medical imaging CT-scan. The reconstruction and the repositioning are key-steps in the elaboration of a 3D model since they affect strongly the accuracy of the final model. This part will explain the reconstruction for each acquisition scale and the step-by-step positioning procedure.

The reconstruction of a 3D model from the medical imaging (figure 3) was realized under the MIMICS software developed by MaterialiseTM. The grey scale DICOM data were binarised with constant threshold of 224 (level used by default for osseous tissues in the software). Thanks to the marching cube algorithm, the surface model of the thorax is then built in a stereo lithography format (triangles edges coordinates and directing facets). The advantage of this standard format is that it can be read by most of CAD software.

The global geometry file is then imported under RAPIDFORMTM software in order to delete the imperfections due to the noise voxels that persisted even after MIMICS thresholding procedure. The main landmark of the thorax is also defined with RAPIDFORMTM and all the geometrical data (from 3D laser scan and μCT) will be repositioned regarding this reference.

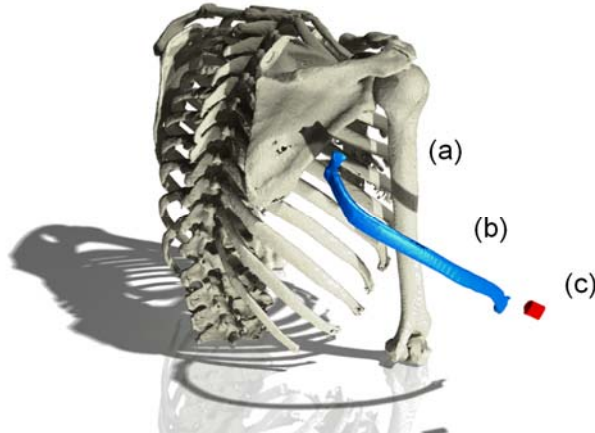


Fig. 2 - 3 Reconstructions Steps - (a) Whole Thorax from CT-Scan, (b) 7th Rib from 3D Maser Scan, (c) 6th μCT Sample from the same Rib.

The 3D laser acquisition, made in step 2, generates automatically a surface model of each rib. This file is then imported in the RAPIDFORM™ software and repositioned correctly in the main landmark (coordinate system) by comparison with the medical imaging 3D model. The repositioning is based on an optimisation loop where the target function consists of minimising the gap between the outer skins of the 2 models. At the end of this merging operation, the cutting edges of μCT samples appeared visible on the whole thorax model. Those edges are used to place accurately data coming from the μCT scan.

Before merging the μCT data with data coming from different scales, some preliminary work is needed in order to differentiate cortical bone from spongy one. For each sample, a set of grey scale images is obtained along the principal direction of the sample (the same one of the rib). Each slice is then transformed to a binary image by applying a grey level threshold. This threshold is chosen to ensure a realistic description of both the spongy and the cortical bones. The crucial effect of the segmentation step on the μCT reconstruction accuracy has already been reported in previous studies (Chaari, 2007; Van Rietbergen, 1995). A special attention was paid for this step with an evaluation of the operator effect. The image processing is performed with CTAnalyser software, from SKYSCAN. The advantage of this software is the possibility to choose and build adaptable regions of interest along the sample height. This feature is particularly interesting for the definition of the cortical inner surface.

Indeed the direct reconstructions of the μCT samples using marching cube algorithm contain the whole structural information of rib: cortical and spongy bones (Chaari, 2009). Since the target is the cortical bone thickness characterisation, considering the spongy bone will lead to heavy files with no useful information for our application. One way to simplify the procedure and to reduce the 3D model numerical size and treatment is to overlook the spongy bone in μCT slices. For each slice, the internal border of the rib is delimited by a B-spline based region of interest. This curve is a manually defined as the limit between cortical and spongy bone. Figure 3 illustrates the two 3D models of the same sample with considering the spongy bone in the first subfigure (2 359 256 faces) and only the cortical bone skins in second one (486 610 faces).

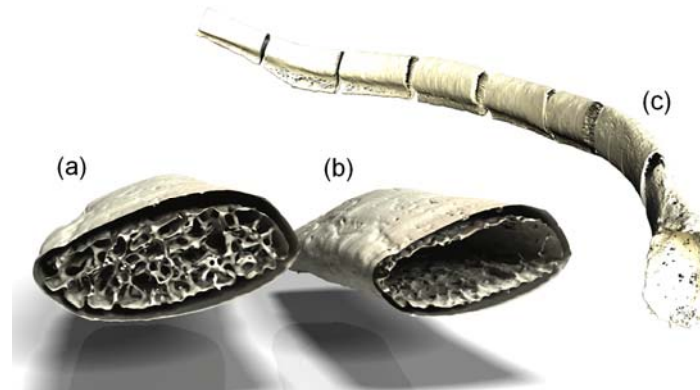


Fig.3 - 3D Reconstructions of μ CT Samples in STL Format (Triangular Facets) - (a) Total Reconstruction with Spongy and Cortical Bone of the 7th μ CT Sample, b) Reconstruction of Cortical Bone of the Same Sample, c) Repositioning of the 8 μ CT Samples of 7th Rib.

In this study, eight 3D samples of rib 7 chosen for this feasibility step were reassembled within the laser scan geometry and the medical CT reconstruction. Figure 4a shows the final eight 3D samples repositioned within the medical CT-scan and 3D laser scan coordinate systems. The shape and curvature of the merged samples is accurate compared to data coming from the CT-scan. The repositioning using two different techniques allows correcting the small imperfections in cutting the sample so that they don't affect the precision of the final model.



Fig.4 - 3D Reconstruction Comparison between Medical CT-Scan and μ CT-Scan, a) μ CT Reconstruction of the 5th μ CT Sample, b) Equivalent Section of the 5th Sample from CT-Scan.

The relevance of using such micro CT acquisitions was assessed regarding the time consumption of this technique. Figures 4a and 4b illustrate 2 reconstructions of the same anatomical area, performed either by the micro CT scanner or the medical imaging. The first fact of this comparison is that the external border (surface) is correctly defined by the both techniques. Obviously the surface of μ CT sample is smoother due to the higher resolution of this technique (20 μ m for μ CT and 800 μ m for CT-scan). Regarding the limit between spongy and cortical bones, the difference is more important: in most parts of the section, CT-scan over estimates cortical bone thickness. Since the average thickness of the rib cortical bone is comparable to the CT precision, 1 or 2 voxels are not sufficient to represent the local variations of this parameter. For the thinner parts, the CT-scan is not able to represent the cortical bone because its thickness is smaller than one voxel.

So, the important advantage of the μ CT is shown in order to generate a geometrical rib model taking into consideration accurately the cortical bone distribution. This comparison highlights also the limits of generating Finite Element Models of the thorax by using only medical imaging.

In order to summarise the acquisition and reconstruction protocol, figure 5 presents the different steps to generate the whole rib with internal and external geometry. This protocol, applied to one rib, takes approximately one week from rib harvesting to the generation of a surface model (STL format). This kind of model, even simplified, is still heavy to handle numerically to be used for FEM and geometrical analysis.

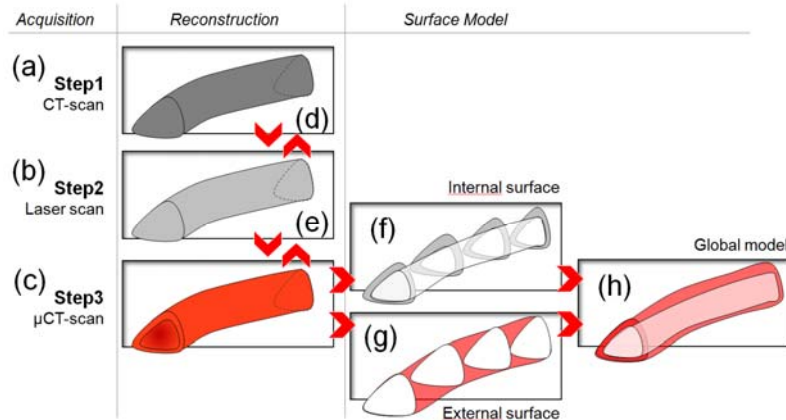


Fig. 5 - Modelling Protocol for One Rib - (1) and (2) Acquisition of the External Geometry, (3) Acquisition of the Internal Geometry, (4) Repositioning of all the Reconstructions, (5) Separation of the Spongy Bone, (6) Generation of the Outer Skin, (7) Merging for the Global Surface Model.

The global model obtained should be transformed to a parametric model consisting of two B-spline interpolated surfaces: a first surface corresponding to the external geometry of the rib and a second one defining the limit between cortical and spongy bone.

III- RESULT

III-1. SURFACIC MODEL GENERATION AND ANALYSIS

The 8 samples juxtaposition in the main coordinate system leads to a STL surface model with discontinuities due to the cutting edges. To overcome this problem and to guarantee the continuity, an interpolated surface was generated in CATIA software from Dassault Systèmes. The first surface defines the external rib geometry from the μCT sample and a second one is created to determine a limit between the cortical and spongy bone. Generating surfaces with B-splines needs to create the rib curvature, thanks to the definition of several normal sections. This chapter will describe the operations necessary for the generation of the surfacic model.

First, a main guiding line of the rib is defined and generated from the STL file. It consists of generating the intersection between 2 surfaces from 4 B-spline curves drawn on the main directions of the rib (figure 6a). Even if this considered curve is not exactly the neutral rib line, its advantage is to be continuous and to permit to configure cutting planes. These planes are normal to the guiding line and the gap between 2 consecutive planes is 2% of the rib length. In THOMO project, the choice of this gap value ensures the best biofidelity in terms of rib geometry. This parameter is also a key-point for the FEM generation, in order to get better results for ribs' geometrical and structural analysis. For future works, this parameter will be conditioned by the mesh refinement of the FEM.

These planes intercept the 2 surfaces of the STL reconstruction at regular intervals. The second step is to create 2 B-spline curves (internal and external) representing intersection between the STL model and each cutting plane (figure 6b). The external curve is perfectly obtained by the border detection of the rib. The internal one is manually defined to simplify the variation of cortical bone thickness along

the rib. An automatic detection of the inner curve is possible and may give better definition of the limit between cortical and spongy bone but it leads to non-continuous curves. The modelling strategy here is based on a surface interpolation of the curve in cutting planes in order to obtain the whole geometry of the rib. That will ensure the modelling accuracy with progressive variation of the bone distribution and especially avoid jumps in cortical thicknesses. So a non-continuous inner curve is not suitable for this study. Even with this approximation, our modelling representation of the rib section is obviously more accurate than previous studies in which the sections are represented by only 2 ellipsoids (Granik, 1973).



Fig. 6 - Surface Reconstruction for 1 μ CT sample - (a) Generation of the Guide Line from 4 B-spline Curve, (b) B-Spline Curve Delimitations for Inner and Outer Surface, (c) Delimited Surface and Sectional Area for 1 Sample.

All these B-spline curves from the different cutting planes are interpolated with continuous surfaces and are used to generate a 3D model that will be used for building the FEM. For geometrical analysis, the 2 B-spline curves in each plane are considered to define the section of the rib.

The final target of this study is to characterise geometrical and structural properties of the ribs. However, the procedure explained here allows, as a first step, performing a fast analysis on the section cuts. **The advantage of this approach is to provide a more detailed and continuous description of bone thickness and inertia properties along the rib compared** to those reported in the literature (Roberts, 1972; Kemper, 2007). This methodology will be applied on different whole PMHS for investigating intra and inter individual dispersions. In order to illustrate the complexity of the bone distribution, the cortical bone thickness is considered in figure 7.

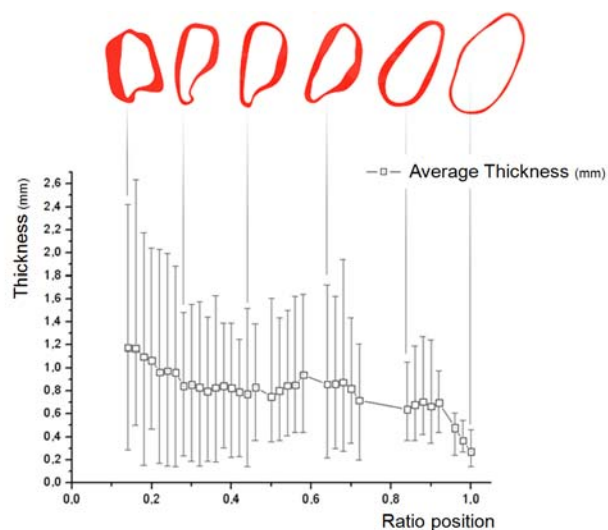


Fig. 7 - Evolution of the Cortical Bone Average, Minimal and Maximal Thicknesses in each Section, between the Head Rib (0%) and the Costochondral Junction (100%).

On the 7th left rib of the first THOMO PMHS, 50 sections were defined along the rib. The rib length is 302 mm, corresponding to a sectional cutting plane every 6 mm (2% gap). Figure 7 presents the thickness variation along the main guiding line. The position is presented in terms of percentage of rib length from 0% which corresponds to the costovertebral junction to 100% which is the costochondral junction. The missing parts from 0 to 14% and for around 80% correspond to the head of the rib and a part which have been used for mechanical testing. In each cutting section, 1000 normal segments are used to define the average and min-max thicknesses.

On each section, a wide dispersion of the cortical thickness is observed. The variations seem to be asymmetrical since the maximum thickness is far from the average. That means that most of the sections have a very thin layer of cortical bone. None of the existing FEM of the human thorax takes into account this characteristic of thickness variation in the same section even if it appears very significant. Regarding the average thickness distribution along the rib, a non-continuous decrease of cortical thickness is observed from the rib head to the cartilage (from 1.2 mm to 0.3 mm). Some of current FE models are able to take into account thickness variation along the rib but are limited to a monotone interval function with a maximum of 5 values along the rib length. THOMO Project aims at obtaining a more biofidelic FE model which will be able to represent the real thickness variation along the rib and in each normal section.

III.2- FINITE ELEMENT MODEL GENERATION

For crashworthiness applications, the virtual human models used by car manufacturers must be as biofidelic as possible with a reasonable computing cost. In existing FE models of the thorax (Robin, 2001; Behr, 2003), the cortical bone in ribs is generally represented by shell elements of 5 mm of average size. The thickness is usually constant or defined by different discrete levels along the rib (generally 3 or 5 average thicknesses). A solid element based modelling would be of course more relevant but the model would be very heavy to handle and difficult to be integrated in a full crash simulation. Since THOMO project goal is to build a biofidelic model for industrial use, shell element representation is the optimised option. The project originality is to describe as well as possible the real thickness distribution of the cortical bone in every part of the thorax. Generating such a model needs the definition of a neutral surface between the internal and external skins of the rib.

Usual CAD software is able to generate neutral surface (average surface) for simple shapes but will not do it correctly considering two complex surfaces. So, it was necessary to develop a new method allowing creating a neutral surface from the two complex surfaces of the rib. This work was realised in a special routine on MATLAB software from The MathWorks. The rib CAD model consisting of interpolated surfaces is imported in MATLAB in STL format. In this format, the surface is described by small triangles indexed by their mesh points and normal vector. Every point and every normal vector is referenced by Cartesian 3D coordinates. Figure 8a gives an idea of the input hyper matrix where all the coordinates are sorted. The developed routine analyses the distances between each meshing point of the internal surface to the other points on the external one (figure 8b). This figure summarises the procedure in 2D which was actually applied in 3D in this study, and all the adjacent points are considered. All the distances are stored in the sorting part of a hyper matrix. At the end of the loop, the minimum distance, with the right orientation is identified. The thickness of the rib in this position is obtained and the program creates a middle point between these selected coordinates. By repeating this loop for all points in 3D coordinates, the neutral surface can be generated by connecting all the middle points.

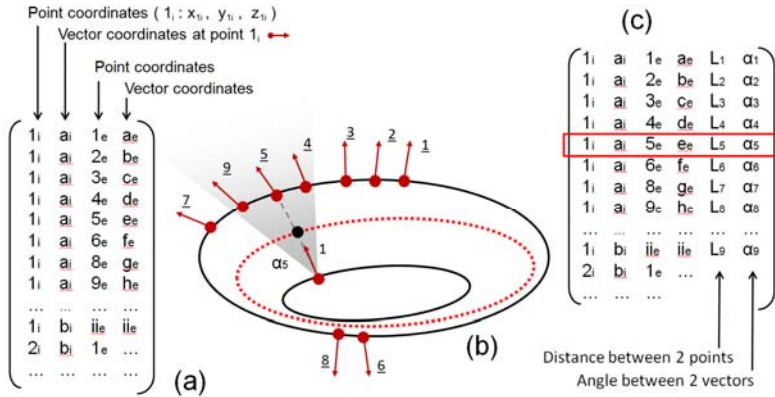


Fig. 8 - Principle of Neutral Surface Generation- (a) Input Matrix from STL file, (b) 2D Scheme of Distances Computing, (c) Output Matrix with Sorted Distances from one Point, the Highlighted Line is used to Create one Point of the Neutral Surface.

The next step of this method is to define a shell meshing with the real thickness variation. The generated neutral surface has generic format and can be imported in any meshing software. In this study, the neutral surface is meshed with 0.5 mm fixed size shell elements, thanks to HYPERMESH software. The result is saved in the PAM-Crash template data format. The considered shell elements size is intentionally undersized in this study in order to obtain the best precision between geometrical representation of FE model and high-quality detection of thin thickness. If larger elements are used, a lack of accuracy will appear not only on the geometrical aspect (highly curved parts are simplified) but also on the thickness gaps in adjacent elements. The element size influence is not studied in this paper but will be the subject of a future work with correlation between experimental and numerical tests.

Once the mesh generated, this file is imported in a second routine in MATLAB in order to assign the right thickness for each shell element. This routine compares the 3D meshing of the neutral surface (nodes and elements) to the data coming from previous surface STL files (internal and external surfaces). The MATLAB routine computes the centroid for each shell element, regarding the 4 nodes. The element thickness is obtained by measuring the distance between the centroid of the element and the 2 skin surfaces. This procedure is very similar to the first explained routine used for the neutral surface generation. The result matrix includes the nodal coordinates, the shell references and the thicknesses for each element. This matrix is transformed to PAM-Crash format for this application. For each element, a specific material card can be defined. For crash application, a micrometer precision will not increase the result accuracy. This is why another routine is developed to simplify the number of material cards. For that, the interval between minimum and maximum thicknesses is divided by a chosen parameter corresponding to the number of wanted material cards. If the thickness of one element is included on one interval, it will be assigned to the corresponding material card.

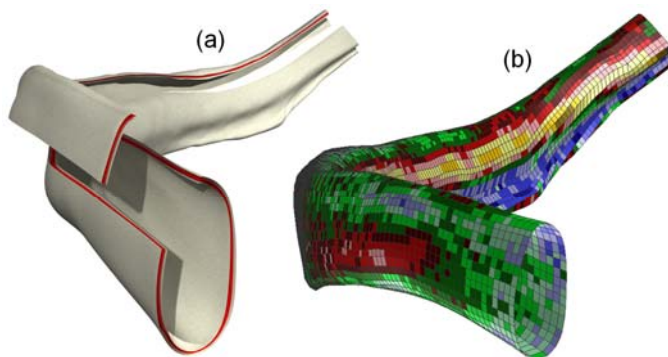


Fig. 9 - (a) Representation of the Rib Neutral Surface, (b) FEM of the Rib (Neutral Surface Meshing with 20 Average Thicknesses).

For the 7th right rib considered in this study, the STL file was define by 110 000 faces (53 170 for external surface and 59 012 for internal one). To generate the neutral surface, the input matrix is approximately composed of 3.109 lines and 12 columns (XYZ coordinates for points and vector to inner and outer surface). This neutral surface is composed by approximately 53 000 points. Once meshed with a 0.5 mm element size, this neutral surface contains 28 000 elements. 20 material cards are chosen for this example (figure 9).

This automatic set of routines generates a finite element model of the rib neutral surface from the complex skins with an innovative use of STL data. The program includes also a parametric configuration to determine material card (thicknesses and bone material properties) to be exported in a PAM-Crash format. This method can be applied to other bone segments such as long bones.

IV- DISCUSSION AND CONCLUSION

The purpose of this study is to develop a new protocol from geometry acquisition to FE modelling of the human thorax with a better precision compare to existing models. This protocol applied on a Post-Mortem Human Subject is a part of THOMO project.

The geometry acquisition strategy is based on a combination of imaging techniques at 3 different scales: a medical CT-scan, a 3D laser scan and a μ CT-scan. The use of different imaging techniques is necessary to obtain a biofidelic FE model with an optimal computing time. The main difficulty in this approach is to combine geometrical models at different resolutions. This issue was figured out by proposing an original method to handle surface models. The work presented in this paper describes the protocol applied on one rib as a feasibility step to be extended to a whole thorax.

In medical imaging, the voxel size resolution is not precise enough to detect the real cortical thickness. Nevertheless, global data coming from this technique are essential for positioning each rib in the thorax and to describe the anthropometry of the subject. μ CT-scan is the optimal method to detect the cortical thickness of the rib and to differentiate a border between cortical and spongy bones. An automatic detection of this inner skin is possible but it leads to heavy models which will be anyway simplified in FE modelling. In this intent, manual B-spline definition is the most suitable solution because it gives continuous surfaces to optimise meshing. 3D laser scan is a good tool to link μ CT geometry to the global model based on CT-scan. The part of the protocol regarding μ CT contour definition can be discussed because it is time demanding and operator dependant since it is manual. The ideal validation of this approach is to estimate the dispersion induced by a set of different operators and compare them to the protocol's global precision.

Another main advance of this study is to use parametric CAD modelling to generate the cutting plans normal to the rib curvature. The sections of the rib located between 2 correctly defined B-splines can be used to analyse thickness and inertia (centre of gravity and moments) variations. The gap between cutting plans is a parametric value that can be adjusted so that the variation along the rib can be defined. This parameter can also be adapted to focus on a specific rib area. As expected, first results on one rib show a non-continuous evolution of the average cortical thickness. The next step is to apply this kind of analysis to a large number of ribs coming from different subjects and to identify an average variation law. This will allow the identification of large variation zones, where cutting planes should be very close, and low variation parts where there is no need to many cutting planes. This approach will simplify the surface generation step and the final FE model.

From the complete geometrical acquisition, a finite element model of the rib was built taking into account the entire geometry and bone distribution. Since the model should be adapted for crash application, shell elements were preferred and their size can be adjusted depending on the required accuracy. A set of average thicknesses is defined and each element was assigned with the nearest thickness. The distribution of thickness intervals is also a parametric value that can be adjusted according to the intended accuracy. The model built is now under validation in order to estimate the

advantages of more realistic thickness distribution of the cortical bone. A simple bending load configuration is applied on the rib with the explicit PAM-Crash code. The first aspect of validation will be based on the comparison of global forces either in case of a constant or a variable thickness. Moreover, the fracture location and shape of these 2 simulations will be compared to experimental observations from THOMO project partners.

Acknowledgment

This study is a part of the THOMO project co-funded by the European Community FP 7th. The authors would like to gratefully thank the European Community, and the different partners involved this project (www.thomo.eu). A special thanks to CEESAR, the lead partner of this project, which provided us with the rib samples. The medical CT scans were obtained through a collaboration between CEESAR, Hôpital Cochin Radiologie B, ENSAM and LAB.

The present research work is also supported by the International Campus on Safety and Intermodality in Transportation (CISIT), the Nord-Pas-de-Calais Region, the Regional Delegation for Research and Technology, the Department of Higher Education and Research, and the National Centre for Scientific Research (CNRS). The authors gratefully acknowledge the support of these institutions.

This work could not have been done without the generous gift of body donors, through the body donation program of the University of Paris. A special thought to all of them.

References

Behr M., Arnoux P.J., Serre T., Bidal S., Kang H.S., Thollon L., Cavallero C., Kayvantash K., Brunet C. - A Human Model for Road Safety: From Geometrical Acquisition to Model Validation with Radioss, *Computer Methods in Biomechanics & Biomedical Engineering*, Volume 6, September 2003, 263 – 273.

Chaari F., Markiewicz E., Drazetic P. - Identification Of The Spongy Bone Mechanical Behaviour under Compression Loads: Numerical Simulation Versus Experimental Results, *International Journal of Crashworthiness*, Volume 12, 2007, 247-253.

Chaari F., Halgrin J., Markiewicz E., Drazetic P. - Spongy Bone Deformation Mechanisms : Experimental And Numerical Studies, *European Journal Of Computational Mechanics*, Volume 18 (1) , 2009, 67-79.

Charpail E., Laporte S., Trosseille X., Valancien G., Lavaste F. - Material and Structure Characterization Of Human Ribs, *Journal of Biomechanics*, Volume 39, 2005, S155-S156

Delille R., Lesueur D., Potier P., Drazetic P., Markiewicz E. - Experimental Study Of The Bone Behaviour Of The Human Skull Bone For The Development Of A Physical Head Model. *International Journal of Crashworthiness*, Volume 12 (2), 2007, 101-108.

Foret-Bruno J-Y., Trosseille X., Le Coz J-Y., Bendjellal F., Steyer C., Phalempin T., Villeforceix D., Dandres P., Got C. - Thoracic Injury Risk in Frontal Car Crashes with Occupant Restrained with Belt Load Limiter, *Stapp Car Crash Journal*, Volume 42, 1998, p-337.

Foret-Bruno J-Y., Trosseille X., Page Y., Huère J-F, Le Coz J-Y., Bendjellal F., Diboine A., Phalempin T., Villeforceix D., Baudrit P., H. Guillemot, J-C Coltat - Comparison of Thoracic Injury Risk in Frontal Car Crashes for Occupant Restrained without Belt Load Limiters and Those Restrained with 6 kN and 4 kN Belt Load Limiters, *Stapp Car Crash Journal*, Volume 45, 2001, p-375.

Granik G., Stein I. - Human Ribs: Static Testing As A Promising Medical Application, *Journal of Biomechanics*, Volume 6, 1973, 237-240.

Kallieris D., Riedl H. - Mechanical tests on bone and cartilage. *Final report of the European project HUMOS*, 2000.

Kemper A., McNally C., Pullins C., Freeman L., Duma S. Rouhana S. – The Biomechanics of Human: Material and Structural Properties from Dynamic Tension and Bending Tests, *Stapp Car Crash Journal*, Volume 51, 2007, p235-273.

Kent R., Lee S-H., Darvish K., Wang S., Poster C., Lange A., Brede C., Lange D., Matsuoka F. - Structural and Material Changes in the Aging Thorax and Their Role in Crash Protection for Older Occupants, *Stapp Car Crash Journal*, Volume 49, 2005, p231-249.

Iwamoto M., Kisanuki Y., Watanabe I., Furusawa K., Miki K., Hasegawa J. - Development Of A Finite Element Model Of The Total Human Model For Safety (Thums) And Application To Injury Reconstruction, *Proceedings of International IRCOBI Conference*, 2002, 31–42.

Li Z., Kindig M., Kerrigan J., Untaroiu C., Subit D., Crandall J., Kent R. - Rib fractures under anterior-posterior dynamic loads: Experimental and finite-element study, *Journal of Biomechanics*, Volume 43, Issue 2, 2009, 228-234.

Lizee E., Robin S., Song E. - Development of 3D finite element model of the human body, *Proceedings of the 42nd Stapp Car Crash Conference*, 1998, 115-138.

Roberts S., Chen P. - Global geometric characteristics of typical human ribs, *Journal of Biomechanics*, Volume 5, 1972, 191-201.

Sandoz B., Laporte S., Charpail E., Trosseille X., Lavaste F. - Influence of the velocity in human ribs response, *Journal of Biomechanics*, Volume 40, Supplement 2, 2007, 215.

Trosseille X., Baudrit P., Leport T., Vallancien G. - Rib Cage Strain Pattern as a Function of Chest Loading Configuration, *Stapp car crash journal 2008*, 2008, 52:205-31.

Van Rietbergen B., Weinans H., Huiskes R., Odgaard A. - A New Method To Determine Trabecular Bone Elastic Properties And Loading Using Micromechanical Finite Element Models, *Journal of Biomechanics*, Volume 28(1), 1995, p69-81.

World Health Organization - World Report on Road Traffic Injury Prevention, Geneva, 2004.

World Health Organization - Global status report on road safety, December 2009.

World Health Organization - First Global Ministerial Conference on Road Safety: Time for Action-Moscow Declaration, Moscow, 19-20 November 2009.

Yoganandan N., Pintar F. - Biomechanics of human thoracic ribs, *Journal of biomechanical engineering*, volume 120, N°1, 1998, 100-104.